

Benchmark for Room Acoustical Simulation (BRAS)

Documentation of the database

Lukas Aspöck, Michael Vorländer
*RWTH Aachen, Institute of Technical Acoustics,
Kopernikusstr. 5, D-52074 Aachen, Germany*
{*las; mvo*}@akustik.rwth-aachen.de

Fabian Brinkmann, David Ackermann, Stefan Weinzierl
*TU Berlin, Audio Communication Group,
Einsteinufer 17c, D-10587 Berlin, Germany*
{*fabian.brinkmann; david.ackermann; stefan.weinzierl*}@tu-berlin.de

September 1, 2020



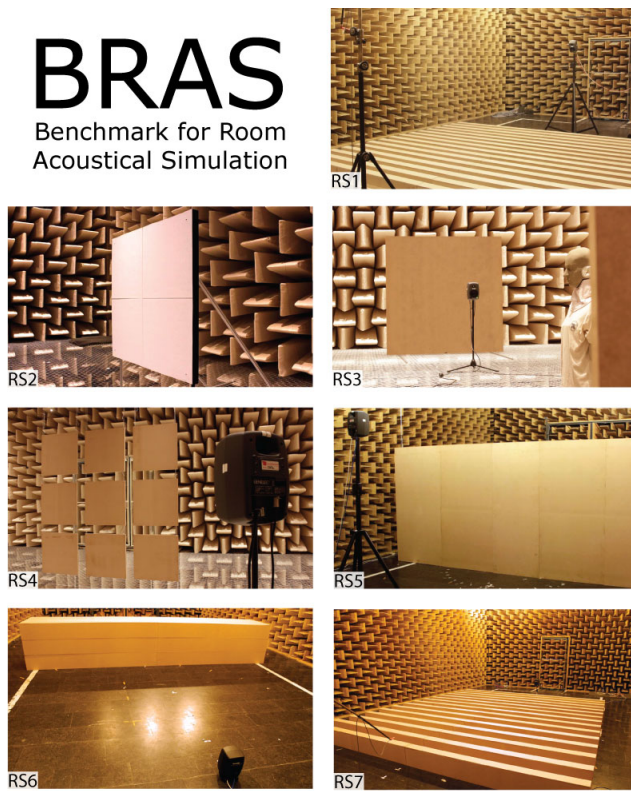


Figure 1: Scenes of the BRAS and its appendix. Numbers refer to Table 2.

2.1 Scene descriptions

The folder `1 Scene descriptions` contains one subfolder for each scene including the scene specific data.

2.1.1 Geometry

The subfolder `Geometry` contains 3D models of the scene saved as SketchUp files and screenshots to gain a quick overview. All files are named according to the scheme `sceneNo_IRtype`, e.g. `CR3_RIR` defines the geometry of the medium room for simulating single-channel room impulse responses, whereas `CR3_BRIR` defines the same room with source and receiver positions for simulating two-channel binaural room impulse re-

sponses. In some cases, a scene is divided into sub-scenes, which is noted by `sceneNo_IRtype_subScene`, e.g. `RS1_RIR_Diffusor`.

Each SketchUp file contains a 3D model of the scene and the names, positions, and orientations of the sources and receivers. Textures are assigned to the surfaces of the 3D models to specify their material, e.g., `mat_RockFonSonarG` (cf. Section 2.3). To view the texture of a surface in SketchUp, use the *Sample Point* option of the *Paint Bucket Tool*. If the object belongs to a group or a component, double click it in the *edit mode* before using the *Paint Bucket Tool*.

Source and receiver positions are marked with 3D icons and text labels that specify the position of the reference points (cf. Section 3.3 and Table 4). The labels are named `LSno_type` for the sources (loudspeakers), and `MPno_type` for the receivers (microphones). For example `LS1_Genelec8020c` gives the position of the scene’s first source, in this case a Genelec 8020c speaker. Directivities according to the labels are located in the corresponding folders (cf. Section 2.2). The correct position and orientation is always given in the label – the positions of the 3D icons might show slight deviations.

Positions are specified with respect to the global coordinate system of the scene where φ [°] gives the orientation in the horizontal plane (x/y plane, $\varphi = 0$ pointing in positive x-direction, $\varphi = 90$ pointing in positive y-direction), and ϑ [°] specifies the elevation ($\vartheta = 90$ pointing in positive z-direction, $\vartheta = -90$ pointing in negative z-direction).

Not all details of the complex rooms could be captured and a list of model simplifications is provided in these cases. Despite this, the models exhibit a high degree of detail and might have to be further simplified for use with geometrical acoustics algorithms. In addition, a model showing the setup of the QSC-K8 speaker is contained in the database for scenes `CR2 – CR4`.

2.1.2 Pictures

The subfolder `Pictures` contains panorama and detail photographs of the scenes including a scale.

2.1.3 Impulse responses

The measured room impulse responses (RIRs) and binaural room impulse responses (BRIRs) are contained in the subfolders `RIRs` and `BRIRs`. They are provided as SOFA files [1] and wav-files with a sampling rate of 44.1 kHz. The SOFA files contain all IRs of one scene and hold additional meta data, while one wav file is given for each IR. In case of the binaural impulse responses, the first wav-file channel holds the left ear data.

The files are named `sceneNo_type_addInfo.type`, e.g., `RS1_RIRs_Rigid.sofa` holds all IRs for the `Rigid` sub-scene of scene 1, whereas the IR for a specific loudspeaker-microphone combination of the same scene

is given in `RS1_RIR_Rigid_LS1_MP3.wav`. For scenes `CR1 - CR4`, RIRs were measured for 4 different orientations of the Genelec 8020c. This is denoted by `LSorientation` as detailed in [Appendix B](#).

Level Calibration

This section describes the level calibration of the measurements. The simulations should be calibrated accordingly.

RIRs: To establish an absolute sound pressure level, the input chain was calibrated with a microphone calibrator. The output chain was calibrated to a free field sound pressure of 80 dB at 1 kHz and a distance of 2 m in front of the loudspeaker, i.e., $\Phi = \Theta = 0^\circ$ ([Figure 3a](#)). Consequently, the RIR unit is Pascal.

BRIRs: Because the BRIRs are intended for auralization and were thus normalized by a single, frequency independent gain factor per scene as detailed in [Section 3.4.2](#). Consequently, the BRIRs are unit-less.

SOFA files

The SOFA files can be read with various [APIs](#) and store the IRs in the field `Data.IR`. The dimensions of `Data.IR` are listed in [Table 1](#) and differ among scenes and IR types (RIR, BRIR). The additional meta data entries `EmitterID` and `ReceiverID` give the order of the IR and specify the source and receiver according to the labels of the 3D models (cf. [Section 2.1.1](#)). E.g., the IRs of loudspeaker 4 and microphone 2 of RS5 are stored in `Data.IR[8,1,:]`. For scenes RS1, RS3, RS5, and CR1, the `ListenerView`, i.e., the head-above-torso orientation, is relative to the source, i.e. `ListenerView = 0` means that FABIAN is directly facing the source. For CR2–CR4, the `ListenerView` is relative to loudspeaker 7 (the center speaker), i.e. `ListenerView = 0` means that FABIAN is facing loudspeaker 7, while loudspeaker 3 and 6 are to its left and right, respectively.

2.2 Source and receiver descriptions

The folder `2 Source and receiver descriptions` contains directivities of all transducers in corresponding subfolders, e.g., `ITA dodecahedron`.

Directivities by means of impulse responses and third octave band spectra are stored in comma-separated value (CSV) files. The file `readDirectivityData.m` can be used for reading the data in Matlab. The directivities are provided on an equal-angle spherical sampling grid with an angular resolution of $1^\circ \times 1^\circ$ in azimuth and elevation, with a total of 64,442 sampling points. Each line in the CSV-files holds the data for one sampling point of the grid as specified in [Figure 2](#) (a, b). Note that different coordinate conventions are used for loudspeaker directivities ([Figure 3a](#)), and head-related impulse responses (HRIRs, [Figure 3b](#)). The coordinate system of the directivities is independent of the

```

1 P000T000,3.1549356,-5.1039181,...
2 P000T001,2.4440977,-6.2950617,...
:
:
64441 P359T179,-1.2831306,-0.8082714,...
64442 P000T180,-1.2037028,-0.7688371,...
```

(a) Impulse response data format.

```

1 f in Hz, 20, 25, ...
2 P000T000,-73.9423324 + 41.6702700i,...
3 P000T001,-74.4630423 + 41.5323030i,...
:
:
64442 P359T179,-21.5571372 + 37.5295540i,...
64443 P000T180,-22.5353947 + 37.6447504i,...
```

(b) 3rd octave spectrum data format.

[Figure 2](#): Format of the directivity data in the front pole coordinate system ([Fig. 3a](#)). Data in the top pole coordinate system are stored in analogy with angles being specified by `A000E+00` ([Fig. 3b](#)).

coordinate system of the 3D models in the SketchUp files.

Source directivities (Genelec 8020c, QSC-K8, ITA dodecahedron)

The source directivities are stored in the front-pole coordinate system, where Φ [P] gives the orientation in the frontal plane (y/z plane, $\Phi = 0^\circ$ pointing in positive z-direction, $\Phi^\circ = 90$ pointing in positive y-direction) and Θ [T] gives the orientation in the median plane (x/z plane, $\Theta = 0$ pointing in positive x-direction, $\Theta = 90$ pointing in positive z-direction). IRs are provided at a sampling rate of 44.1 kHz, and third-octave band magnitude/phase spectra (MPS) from 20 Hz to 20 kHz:

```
LoudspeakerName_1x1_64442_IR_front_pole.csv
LoudspeakerName_1x1_64442_MPS_front_pole.csv
```

Note that the on-axis impulse/frequency response is included in the files, i.e., the directivities were not normalized to frontal sound incidence. The on-axis responses must be included in the simulation to match the measurements without further normalization.

Separate directivities were measured for the mid and high frequency unit of the ITA dodecahedral speaker, while the low-frequency unit is specified by a single frequency response, i.e. it should be modeled as omnidirectional. For detailed investigations, separate simulations for the three units can be considered. The cross-over frequencies coincide with octave cut-off frequencies (cf. [Section 3.3.1](#)). The dimensions of the components are given in:

```
ITA_dodecahedron_model_description.skp
ITA_dodecahedron_model_description.png.
```

#	Type	Data.IR	Dimensions	Meta data
RS1–RS7	RIR	$M \times R \times N$	M: Number of IRs R: 1 N: IR duration [samples]	M: EmitterID, ReceiverID R: - N: -
CR1–CR4	RIR	$M \times R \times E \times N$	M: Measurements (for each R, E) R: Microphone pos. E: Loudspeaker pos. N: IR duration [samples]	M: MeasurementView R: ReceiverID E: EmitterID N: -
RS1–RS7 CR1–CR4	BRIR	$M \times R \times E \times N$	M: Number of HATOs R: 2 (left, and right ear) E: Loudspeaker pos. N: IR duration [samples]	M: ListenerView R: ReceiverID E: EmitterID N: -

Table 1: Data format of IRs stored in the field `Data.IR` inside the SOFA files. The column **Meta data** specifies the SOFA field that determines the IR order.

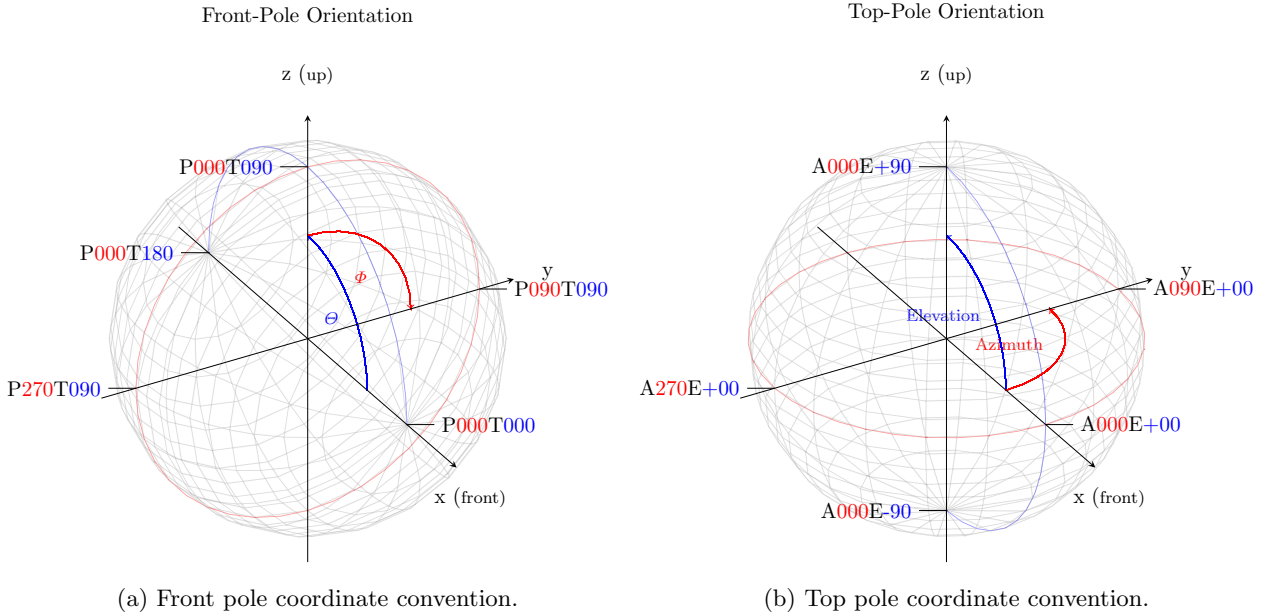


Figure 3: Coordinate conventions of the directivity data.

Receiver directivities (FABIAN Head-related impulse responses – HRIRs)

The HRIRs are provided in the top pole coordinate system, where the azimuth φ [A] gives the orientation in the horizontal plane (x/y plane, $\varphi^\circ = 0$ pointing in positive x-direction, $\varphi^\circ = 90$ pointing in positive y-direction) and the elevation ϑ [E] gives the orientation in the median plane (x/z plane, $\vartheta^\circ = 0$ pointing in positive x-direction, $\vartheta^\circ = 90$ pointing in positive z-direction). The HRIRs are provided as 256 sample IRs at a sampling rate of 44.1 kHz. Separate files are provided for the left (L) and right (R) ear, and different head-above-torso orientations (HATOs). A HATO of 10° denotes a head rotation of ten degree to the left, and a HATO of -10° denotes a head rotation of ten degree to the right:

HATO_10_1x1_64442_HRIR_L_top_pole.csv
HATO_-10_1x1_64442_HRIR_L_top_pole.csv

3D surface meshes of FABIAN's for HATO = 0° are provided for wave based BRIR simulations:

FABIAN_6k_HAT00.stl: Average edge lengths 2 mm, 10 mm, and 10 mm for the pinnae, head, and torso. Valid up to ≈ 6 kHz.

FABIAN_22k_HAT00.stl: Average edge lengths 2 mm, 2 mm, and 10 mm for the pinnae, head, and torso. Valid up to ≈ 22 kHz.

Meshes for HATOs between $\pm 50^\circ$ with a resolution of 10° are contained in the FABIAN database [2].

2.3 Surface descriptions

The folder `3 Surface descriptions` contains information about the materials contained in the scenes. An overview of the materials is given in the file

`MaterialOverview.pdf`. Each material’s characteristic is defined in a csv file (see folder `_csv`), a short documentation in a corresponding text file (see folder `_descr`), a figure showing the absorption and scattering values (see folder `_plots`), and an image of the corresponding surface (see folder `_img`). The csv-files contain three lines, of which the first holds the frequency, the second the absorption coefficients, and the third the scattering coefficients. The `_csv` folder contains two subfolders `initial_estimates`, and `fitted_estimates`. The absorption coefficients in the latter were fitted to the measured reverberation times based on Eyring’s formula [3] and the initial estimates (cf. Section 3.2.1). Fitted values are only available for the complex rooms (CR1-CR4), because the surface descriptions for the remaining scenes could be measured with high precision.

While the materials that were used in the reference scenes (RS1-RS7) have their individual documentation, only one documentation file for all materials inside the complex rooms (CR1-CR4) is given, and named correspondingly. The scene descriptions, provided in the `*.skp` files, indicate which material should be used for the surfaces of the scene (cf. Section 2.1.1).

2.4 Additional data

The folder 4 **Additional data** contains material for comparing simulated and measured impulse responses. Room acoustical parameters in third octaves were calculated using the ITAtoolbox [4] and saved as comma-separated values. A Matlab script for loading the impulse responses and calculating the parameters is also available. This is intended for a physical comparison of measured and simulated impulse responses. Moreover, a short excerpt of an anechoic string quartet recording and binaural auralizations of scenes CR2–CR4 are included in the database. These files are intended for a perceptual comparison of measured and simulated impulse responses.

3 Acquisition of the database

A tabulated summary of the scenes contained in the BRAS and the equipment that was used to collect the data can be found in Tables 2 and 3. All measurements and scene setups were supervised and processed by authors LA, FB, and DA. To assure consistency across the data of different scenes, a standardized protocol, identical equipment, as well as identical measurement and post-processing scripts were used that only differed with respect to the length of the sine sweeps and final impulse responses, which were both adjusted to the level of reverberation and background noise. All acoustic measurements were conducted with a sampling rate of 44.1 kHz, and all impulse responses were obtained by swept sine measurements and spectral deconvolution [5].

3.1 Geometry

Generating the scene geometry can be split in two parts: The acquisition of the room geometry, and positioning the objects inside the room. The latter was done relative to a predefined reference point with the help of self leveling cross line lasers (Bosch Quigo, precision ± 0.8 mm/m), a laser distance meter (Bosch DLE 50 Professional, precision ± 1.5 mm), and a laser angle measurer (geo-FENNEL EL 823, equipped with a Hama LP-21 laser pointer, precision $\pm 0.5^\circ$). The reference points for positioning the sources and receivers are listed in Table 4. They are identical to the center of rotation during the directivity measurements (cf. Section 3.3.1 and 3.3.2).

Reference scenes. In RS2–4, the objects had to be placed on the wire-woven floor of the fully anechoic chamber. Because the floor’s inclination slightly changed due to the weight of the objects, the positions were iteratively adjusted with the help of a plumb bob and a remote camera until the objects were perpendicular to the floor. Moreover, the weight of the objects was distributed to a larger area using stands (RS2 & 3), or objects were hung from the ceiling (RS4). In addition to using laser distance meters, the precision of placing the objects within the scene was verified by estimating the direct sound arrival time from the ten times up-sampled measured impulse responses (IRs) by means of threshold based onset detection [6]. A comparison of the acoustically estimated arrival times to the geometrical values given in the scene descriptions showed absolute differences of up to 2.3 cm (1.6 cm on average) for RS1 and 5–7, and 5.5 cm (3.4 cm on average) for RS2–4. Even for the smallest source-to-receiver distance of 3 m and the largest observed errors of 5.5 cm, this would cause magnitude errors of maximally $20 \log_{10}(3.055/3) = 0.16$ dB between the intended and actual sound pressure level, and angular displacements of maximally $\arctan(0.055/3) = 1^\circ$ between the intended and actual source/receiver positions under the assumption of a receiver in the far field of a point-like source. Considering the Genelec 8020c speaker with a woofer-to-tweeter distance of 11 cm, and 3 m source-to-receiver distance, the assumptions above appear to be valid.

Complex rooms. For scenes CR1–3, the room geometry was acquired by manually measuring the positions of corners and important points with a TOPCON EM-30 laser distance meter (precision ± 3 mm) mounted on a VariSphear scanning microphone array [7]. The laser distance meter could be rotated in azimuth and elevation using two computer controllable motors (Schunk PR070, minimum step width 0.001°). For CR2, all points could be scanned from a single position, while some points were blocked in the remaining scenes. In these cases, the rooms were scanned from different positions, and duplicate points were used to align the point clouds. Euclidean distances between duplicate points were smaller than 1.4 cm (7 mm on

#	Name	Date	Location	RIR	BRIR	Meters
BRAS: Reference scenes						
RS1	simple reflection (infinite plate)	Nov. 2015	RWTH Aachen	3/3 (S1, R1, C1, C2, C4)	1/1 (S1, R3, C3, C4)	(M1, M2)
RS2	simple reflection and diffraction (finite plate)	Dec. 2015	TU Berlin	6/5 (S1, R1, C1, C2, C5)	-/-	(M1, M2, M3)
RS3	multiple reflection (parallel finite plates)	Dec. 2015	TU Berlin	1/1 (S1, R1, C1, C2, C5)	1/1 (S1, R3, C3, C4)	(M1, M2)
RS4	single reflection (reflector array)	Dec. 2015	TU Berlin	6/6 (S1, R1, C1, C2, C5)	-/-	(M1, M2, M3)
RS5	diffraction (infinite wedge)	Nov. 2015	RWTH Aachen	4/4 (S1, R1, C1, C2, C4)	1/1 (S1, R3, C3, C4)	(M1, M2)
RS6	diffraction (finite body)	Dec. 2016	RWTH Aachen	3/3 (S1, R1, C1, C2, C4)	-/-	(M1, M2)
RS7	multiple diffraction (seat dip effect)	Dec. 2016	RWTH Aachen	2/4 (S1, R1, C1, C2, C4)	-/-	(M1, M2)
Appendix: Complex rooms						
CR1	coupled rooms (lab. & reverb. chamber)	Nov. 2015	RWTH Aachen	2/2 (S1, S3, R2, C1, C2, C6)	2/2 (S1, R3, C3, C4)	(M1, M2, M4)
CR2	small room (seminar room)	Nov. 2015	RWTH Aachen	2/5 (S1, S3, R2, C1, C2, C6)	5/1 (S2, R3, C3, C4)	(M1, M2, M4)
CR3	medium room (chamber music hall)	Dec. 2015	Konz- erthaus, Berlin	3/5 (S1, S3, R2, C1, C2, C6)	5/1 (S2, R3, C3, C4)	(M1, M2, M4)
CR4	large room (auditorium)	Dec. 2015	TU Berlin	2/5 (S1, S3, R2, C1, C2, C6)	5/1 (S2, R3, C3, C4)	(M1, M2, M4)

Table 2: Overview of the scenes contained in the BRAS and its appendix. Columns *RIR* and *BRIR* give the number of source/receiver positions and the used hardware in parentheses (cf. Table 3).

#	Type	Manufacturer	Model
Sources			
S1	Loudspeaker	Genelec	8020c (2-way active studio monitor)
S2	Loudspeaker	QSC	K8 (2-way active PA speaker)
S3	Loudspeaker	RWTH Aachen	3-way dodecahedron loudspeaker, with FourAudio HD2 loudspeaker management system
Receiver			
R1	Microphone	G.R.A.S.	40AF 1/2" free-field capsule
R2	Microphone	Bruel & Kjør	Type 4134 1/2" diffuse-field capsule
R3	Microphone	TU Berlin	FABIAN head and torso simulator, with DPA 4060 microphones
Converters			
C1	Microphone	Bruel & Kjør	Type 2669-B 1/2" microphone preamplifier
C2	Preamplifier	Bruel & Kjør	Type 2692-A-011 Nexus charge amplifier
C3	Preamplifier	Lake People	C360 2-channel microphone preamp
C4	Audio interface	RME	Multiface II with HDSP cardbus
C5	Audio Interface	RME	Fireface UC
C6	Audio Interfaces	RME	Digiface (HDSP cardbus) with OctaMic preamp
Positioning tools			
M1	Cross line laser	Bosch	Quigo (claimed accuracy ± 0.8 mm/m)
M2	Laser distance meter	Bosch	Bosch DLE 50 Professional (claimed accuracy ± 1.5 mm)
M3	Laser angle meter	geo-FENNEL	EL 832 (claimed accuracy $\pm 0.5^\circ$, equipped with Hama LP-21 laser pointer)
M4	Room scanning system	TH Cologne	VariSphear (claimed accuracy $\pm 0.02^\circ$, equipped with Topcon EM-30 laser distance meter)

Table 3: Hardware used for the acquisition of the BRAS. See Table 2 for a list of used hardware per scene.

Device	Reference point
Genelec 8020c (loudspeaker)	Point on the front panel midway between the outmost position of the low/mid frequency driver and the tweeter
QSC-K8 (loudspeaker)	Point on the protective grid in front of the tweeter
Dodecahedron (loudspeaker)	Low-frequency unit: center of circular opening; Mid-frequency unit: center of sphere; High-frequency unit: center of sphere
B&K type 4134 G.R.A.S. 40AF (microphones)	Point on the center of the protective grid in front of the membrane
FABIAN (dummy head)	Interaural center, defined as the midpoint of the line that connects the entrances of the two ear channels

Table 4: Definition of the reference points that define the positions of the sources and receivers. The orientation of the transducers is documented in the database separately for each scene.

average). A check for planarity of the major room surfaces (walls, floor, ceiling) was done by fitting a plane through the points of each surface. Mean absolute deviations in direction of the surface normal of 2.6 cm were corrected by moving the points on to the surface. Maximum deviations of 6 cm and 8.5 cm occurred in two cases in the reverberation chamber (CR1) where the corner points were not clearly defined and for a wall that showed small irregularities. Since the reverberation chamber only serves as the coupled volume for the main room of CR1, this outlier seems less relevant. In addition, the RMS Hausdorff distance between the non-planar and planar surfaces was calculated for the walls floor and ceiling using METRO [8], with an average across rooms of 7.8 mm and the largest difference of 3.8 cm again found for the reverberation (CR1). Afterwards, the 3D modeling software SketchUp was used to design the final room model based on the post-processed point clouds.

Due to the complexity of scene CR4, the initial room model was based on architectural drawings and validated against a set of 15 manually measured distances between relevant points in the room (e.g. the height width and depth at different positions in the room). Deviations between measured and initially modeled distances were smaller than 52 cm and 20 cm on average, and the model was corrected according to the measurements by adjusting the position of the floor, ceiling and walls. In a final step, material names were assigned to each surface in the room models using SketchUp, and the positions and orientations of the sources/receivers were inserted.

The geometry acquisition aimed at obtaining a higher level of detail than the resolution of 50 cm typically used for GA simulations [9, p. 176]. The mod-

els thus include structures that might have to be simplified depending on the need of the simulation algorithm. Nevertheless, not all details of the complex rooms (CR1–4) were captured, and the final models are accompanied by a list of model simplifications and pictures that show the omitted details (cf. Section 2.1.1). Not modeled were, for example, handrails and cable ducts with diameters of a couple of centimeters, stucco ornamentation, projections on walls with a depth of a couple of centimeters, and chandeliers.

The additional check of the positioning precision by means of onset detection could not be done for CR1–4, because i) the Genelec loudspeaker was not facing the receivers, and ii) the dodecahedron source consists of multiple drivers, which substantially widens the direct sound impulse and caused errors in the onset detection. However, the positioning was done in analogy to scenes RS1 & 5–7 using lasers, and it is thus reasonable to assume that the positioning accuracy is comparable to that of scenes RS1 & 5–7.

3.2 Surface descriptions

As mentioned in the introduction, it is challenging to provide high precision boundary conditions for room acoustical simulations. For this purpose, absorption coefficients of the reference scenes RS1–7 were measured in situ, whereas they were derived from a combination of measurements and tabulated values of similar materials for the complex rooms CR1–4, where they can be considered as a best practice approximation. In total, the database contains 28 surface materials, stored in 37 data files including absorption and scattering coefficients in third octaves from 20 Hz to 20 kHz. Multiple files are available for some materials providing data for different angles of incidence.

3.2.1 Absorption coefficients

Reference scenes. For RS1–7, three materials were used and described for different configurations. These include the floor tiles of the hemi anechoic chamber, stone wool absorber tiles, and three medium density fiberboards (MDF) with a thickness of 12 mm (8.91 kg/m²) and 25 mm (15.53 kg/m², and 18.56 kg/m²), which were used to build the reflecting and diffracting objects in RS1–7. An overview of all materials and the applied acquisition methods including the valid frequency ranges is shown in Table 5.

Normal incidence absorption coefficients were measured according to 10534-2 [10] using a circular impedance tube with a diameter of 2 inch. Transfer functions were determined for four microphone positions with distances from the first to the second, third and fourth microphone of 17 mm, 110 mm and 510 mm, respectively. All transfer functions were measured by moving one probe microphone to the desired positions on the mid-axis of the circular tube. Crossover frequencies for the transfer functions between the first (H_{14})

Material	Absorption coefficient acquisition method (valid freq. range)	Scenes
Medium density fiberboard	ISO 10534-2, normal incidence (100 Hz to 4 kHz)	RS1–7
Stone wool absorber	ISO 10534-2, normal incidence (100 Hz to 4 kHz),	RS1–2
Stone wool absorber	Angle dependent in situ measurement (300 Hz to 15 kHz)	RS1–2
Wooden diffusor	Angle dependent in situ measurement, (500 Hz to 15 kHz)	RS1
Tiles of hemi anechoic chamber	Estimated random incidence values (see text)	RS1, 5–7
Room surfaces (24 materials)	Estimated random incidence values (see text)	CR1–4

Table 5: Surface materials of the BRAS database indicating the applied absorption coefficient acquisition method and the scenes in which the corresponding materials were used.

and the second microphone pair (H_{13}), and between the second (H_{13}) and the third microphone pair (H_{12}), were defined at 900 Hz and 1200 Hz, respectively. The measurements are valid above 100 Hz due to the limited frequency range of the loudspeaker, and below 4 kHz due to the diameter of the tube [10].

Angle-dependent absorption coefficients of the stone wool absorber and the diffusor were determined using the setup and measurements of RS1. In the impulse response measurements of the rigid floor, the diffusor and the absorber, the reflection was isolated as described by Mommertz [11] for four $\phi_{in} - \phi_{out}$ combinations. This was done by a two-sided Hann window (0.6 ms fade in, 1.8 ms fade out, cf. Fig. 4, top). The reflection factors were then obtained by spectral division, referencing the windowed impulse responses of the absorber and diffusor to the rigid floor (cf. Fig. 4, middle). The absorption coefficients were determined from the absolute value of the reflection factors, smoothed with a one-third octave sliding window (cf. Fig. 4, bottom). This was done for the symmetric source/receiver setup (specular reflection) for the angles $\phi_{in} = \phi_{out} = \{30^\circ, 45^\circ, 60^\circ\}$ based on the impulse responses of the omnidirectional receiver, and for $\phi_{in} = 45^\circ, \phi_{out} = 32^\circ$ based on the binaural data. For other combinations of ϕ_{in} and ϕ_{out} , no measured data is provided, but can be processed from the provided measured impulse responses of scene RS1. The lower frequency limit of this method differs for the two measured materials due to edge effects (cf. Table 5). Above 15 kHz, minor differences of source, receiver, and probe positions affect the measured result. Miss-

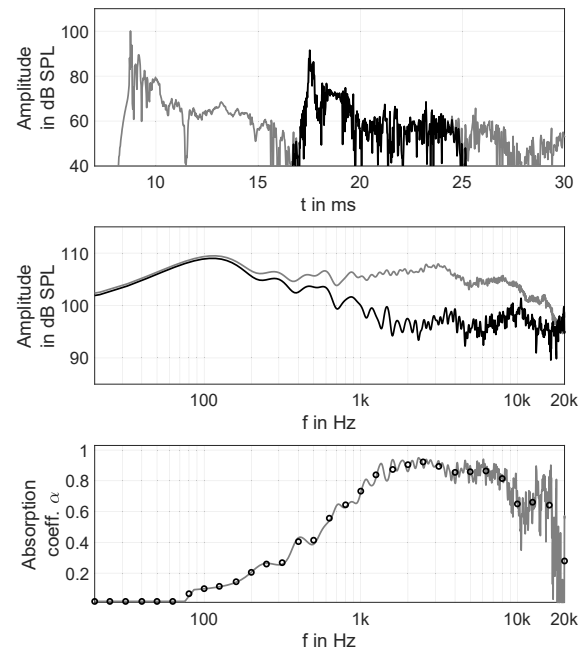


Figure 4: Generation of the angle dependent absorption coefficient for the example of the absorbing setup and angles $\phi_{in} = \phi_{out} = 30^\circ$. Top: Windowed (black) and full length impulse response (gray) of the absorbing setup. Middle: Frequency responses of the absorbing (black) and rigid (gray) reflection calculated from the windowed impulse responses. Bottom: Unsmoothed (gray) and final (circles) absorption coefficients α obtained after 3rd octave smoothing

ing values below and above the valid frequency ranges were linearly extrapolated or attributed from tabulated values of similar materials [9, 12]. The absorption data of the stone wool absorber obtained in this way is consistent with other measurement results using ISO 354 and ISO 10534-2 for random-incidence and normal incidence, respectively, considering angle-dependent effects such as an increase of absorption for an increasing angle of incidence.

The absorption of the tiles of the reflective floor of the hemi anechoic chamber (RS1, 5–7) can be described by an almost frequency independent absorption coefficient with an average value of less than 0.02.

Complex rooms. For scenes CR1–4, several surfaces were initially measured with a hand-held in situ device [13], consisting of a loudspeaker in a spherical enclosure and a combined sensor unit measuring sound pressure and particle velocity [14]. This method can deliver valid results for normal incidence if applied for porous absorbers in controlled scenarios, but faces several challenges otherwise. These include high uncertainties for reflective surfaces and repeated measurements as well as small and complex objects such as chairs. For these reasons the absorption data was derived from in-situ measurements whenever possible and attributed from material databases otherwise [9, 12] (cf. Section 2.3). Less important materials and small

surfaces were disregarded, which lead to four, five, seven, and eight different materials for scenes CR1–4, respectively. Examples for left out surfaces are small doors far away from all source/receiver positions and stucco ornamentation. These sets of coefficients were termed *initial estimates*.

To allow a comparison with the results of RR-I–III and the common practice of room acoustical simulation, a second set of *fitted estimates* is provided for the materials of CR1–4. These were fitted to the measured reverberation times by multiplication with the ratio $\bar{\alpha}/\bar{\alpha}'$ for each third octave band and scene, i.e., the same ratio was applied for all materials within a scene. $\bar{\alpha}$ denotes the average absorption coefficient in CR1–4 calculated under the assumption of a diffuse sound field by solving the Eyring reverberation time for $\bar{\alpha}$

$$T_{\text{Eyring}} = 0.161 \frac{V}{-S \ln(1 - \bar{\alpha}) + 4mV}, \quad (1)$$

(V : room volume according to [Appendix: Complex rooms](#); m : air attenuation [3]). The average absorption coefficient of the initial estimates $\bar{\alpha}'$ was calculated using

$$\bar{\alpha}' = \frac{1}{S} \sum_i S_i \alpha_i' \quad (2)$$

where the surface area $S = \sum_i S_i$ occupied by each material was taken from the 3D room models.

3.2.2 Scattering coefficients

As GA based simulation algorithms commonly take into account non-specular reflections, the BRAS also includes random-incidence scattering coefficients for most materials. Although ISO 17497-1 [15] and ISO 17497-2 [16] describe standardized measurements of random-incidence scattering and directional diffusion, material samples in the required size could not be removed from the rooms. The scattering coefficients of the database were therefore estimated [17] based on the characteristic depth d_{char} [9] of the material in order to provide a transparent calculation model

$$s(f) = 0.5 \cdot \sqrt{\frac{d_{char}}{c/f}}, \quad (3)$$

with c being the speed of sound and f the frequency. As the scene geometries also contain large flat surfaces, the lower limit of $s(f)$ was chosen as 0.05, the upper limit was set to 0.99. The structural depth of all materials is listed in the corresponding material description files. The resulting scattering data for the 31 one-third octave center frequencies between 20 Hz and 20 kHz are provided for all materials, except for the wooden diffuser (RS1), as for this scenario, the modeling of scattering effects of the diffuser is subject of the investigation.

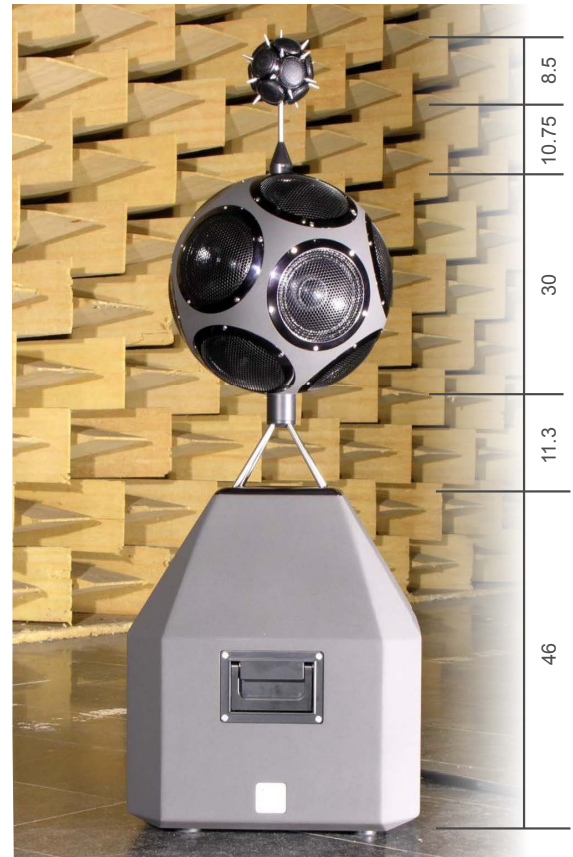


Figure 5: Picture of the DSP driven 3-way dodecahedral speaker. Measures are given in cm. A detailed 3D model is contained in the database (cf. Section 2.2).

3.3 Source and receiver descriptions

3.3.1 Source Directivities

The directivities of the Genelec 8020c, QSC K8, and the dodecahedral speaker were measured in the hemianechoic chamber at RWTH Aachen University on a 2×2 equi-angular top pole sampling grid (Fig. 3b, right) using exponential sweeps (16,384 samples ≈ 0.4 s @ 44.1 kHz sampling rate). The sweep length was sufficient to obtain a peak-to-tail SNR of approximately 80 dB (cf. Fig. 7). The dodecahedral speaker is a custom DSP driven 3-way system with a single low-frequency driver and mid/high-frequency units consisting of 12 speakers in spherical enclosures (cf. Fig. 5). The cross-over frequencies of 177 Hz and 1.42 kHz were chosen according to the upper cut-off frequency of the 125 Hz and 1 kHz octave bands. It was preferred over commercially available 1-way systems because the small high frequency drivers ensure smaller deviations from omnidirectionality than observed with conventional systems [18, 19]

Due to mechanical restrictions, two different systems were used for rotating the transducers: The Genelec 8020c and the dodecahedral speaker were placed on a turntable that controlled the azimuth at a height of 2 m above the ground. The elevation was controlled

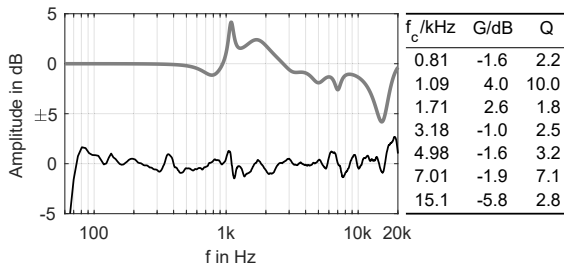


Figure 6: Equalized on-axis magnitude response of the QSC-K8 speaker (black), equalization (gray), and equalizer settings (center frequency, gain, quality). $Q = f_c/|f_2 - f_1|$, where f_1 , and f_2 are the two frequencies with a magnitude of $G/2$ dB (*midpoint dB gain* definition of the bandwidth according to Bristow-Johnson (1994) [20].)

by an arm that was equipped with a G.R.A.S. 40AF half inch free-field microphone at a distance of 2 m from the speaker. To maintain a sufficient time delay between the direct sound and the floor reflection, the lower hemisphere of the loudspeaker directivities was measured after flipping them about the reference points (cf. Tab. 4). For both hemispheres, an overlapping region of 4° below the equator was measured for validation. Differences in one-third octave bands between repeated measurements were below 1 dB, except for some directions behind the Genelec 8020c with low emitted energy. Overall, mean absolute differences of 0.5 dB (SD 0.6 dB) were observed in the overlapping region for third octaves above 1 kHz. In case of the dodecahedral speaker, separate directivities were measured for the mid-frequency and high-frequency unit, in both cases for the full physical setup of the 3-way system (cf. Fig. 5), each referenced to the center of the corresponding unit. The low-frequency unit was modeled omnidirectional because the wavelength at the upper cut-off frequency (1.94 m; 177 Hz) is more than four times larger than the enclosure (0.46 m high). The QSC K8 was rotated using the ELF loudspeaker measurement system (Four Audio) with the microphone placed flush with the floor of the hemi-anechoic chamber at a distance of 8 m. All equalizer settings of the speakers were disabled for reproducibility. Parametric equalizers were used, both in the directivity measurement and in the measurement of the BRIRs, to compensate the free-field on-axis frequency response of the QSC-K8 speaker within a tolerance of ± 3.5 dB to provide an uncolored on-axis frequency response during auralization (cf. Fig. 6 and Section 3.4.2).

The measurement distances were chosen in agreement with the far field criteria $r \gg l$ and $r \gg fl^2/c$ [21, p. 102], where r is the measurement distance, l the acoustically effective source dimension (tweeter-to-woofer distances of 0.11 m and 0.3 m for the Genelec 8020c and QSC-K8, diameters of 0.3 m and 8.5 cm for the Dodecahedron mid and high frequency units),

f the upper frequency limit (16 kHz for the Genelec 8020c, QSC-K8, and Dodecahedron high frequency unit; 1.42 kHz for the Dodecahedron mid frequency unit), and c the speed of sound (343 m/s).

In post-processing, the common propagation delay was removed and a subsonic high-pass filter was applied (4th order Butterworth -3 dB @ 30 Hz). Due to the different mechanical measurement setups and temporal behaviours, IRs were truncated to 9.5 ms (Genelec), 13.6 ms (dodecahedron), and 80 ms (QSC) to discard reflections by applying a 2 ms Hann window fade in/out (cf. Fig 7). In case of the Genelec speaker, the truncation distorted the magnitude response below 200 Hz. To account for this, the magnitude spectrum of a single on-axis measurement – done in the fully anechoic chamber at TU Berlin – was fitted to the truncated IRs by applying a linear fade between 200 Hz and 300 Hz in the frequency domain (gray lines in Fig. 7). The phase response did not suffer from the truncation and was thus left unchanged, i.e., was taken from the truncated IRs. The substitution of only the magnitude response is similar to the combination of near-field and far-field loudspeaker measurements [22]. As a consequence, the final Genelec directivity is omnidirectional below 200 Hz. Since the originally measured data (before windowing) showed deviations from omnidirectionality of less than 1 dB below 200 Hz, this was neglected.

In a final step, separate spherical harmonics interpolations (Eq. (3.26) and (3.31) in [23]) of the magnitude and unwrapped phase spectra with a spherical harmonics order of 20 were used to increase the spatial resolution and to harmonize the sampling grids, which differed across the systems used for the directivity measurements. Differences before and after the interpolation were smaller than 0.4 dB below 10 kHz, and never exceeded 1 dB. The final data are available as impulse responses and complex one-third octave spectra on a $1^\circ \times 1^\circ$ equal angle front pole sampling grid (cf. Fig. 3a).

3.3.2 Receiver Directivities

Two types of receivers were used during the acquisition of the database. Impulse responses with omnidirectional receivers were measured either with diffuse field or free field compensated half inch capsules, Brüel&Kjær type 4134 and G.R.A.S. 40AF, respectively, both using Brüel&Kjær 2669-B microphone preamplifiers. They are supposed to be modeled as omnidirectional receivers in the simulation.

The binaural impulse responses were measured with the FABIAN head and torso simulator, with acoustically measured head-related impulse responses (HRIRs) taken from the open access FABIAN database [24, 2]. It contains HRIRs for 11 different head-above-torso orientations (HATOs), i.e., head rotations to the left and right in steps of 10° covering the typical range of motion of $\pm 50^\circ$ [25]. To ensure

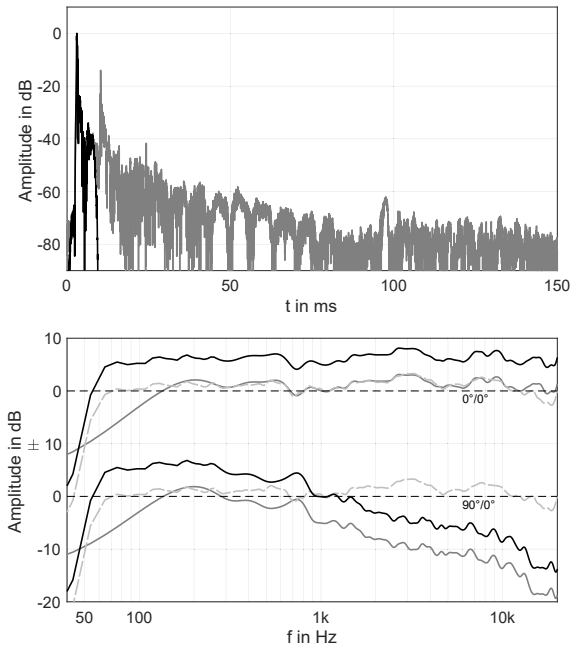


Figure 7: Processing of the Genelec 8020c directivity data. Top: Impulse response for the frontal direction ($0^\circ/0^\circ$) before (gray) and after windowing (black). Bottom: Final frequency responses after spherical harmonics processing (black) in front ($0^\circ/0^\circ$) and to the side ($90^\circ/0^\circ$). The measured directivity after windowing (gray) and the single on-axis measurement that was used below 200 Hz (dashed) are given for validation. Data are 12th octave smoothed to improve the visibility.

that head movements can be auralized without perceivable degradation, HATOs with a resolution of 2° (threshold from [26]) were interpolated ([27], original phase, frequency domain, torso interpolation) using AKtools for Matlab [28]:

```
AKhrirInterpolation(A, E, HATO,
'measured_sh').
```

3.4 Impulse Responses

3.4.1 Omnidirectional Receivers

Impulse responses were measured using exponential sweeps (262,144 samples \approx 6 s @ 44.1 kHz sampling rate) and averaged across four repeated measurements to increase the SNR. A high frequency amplitude reduction that can occur when averaging room impulse responses was not observed [29], with deviations between reverberation times (T_{20} @ 4 kHz and 8 kHz) of averaged and single impulse responses always smaller than 1.4% and 0.4% on average. The microphones were always oriented towards the current sound source position, corresponding to the 0° direction as defined by the manufacturers. The input measurement chain was calibrated using a B&K Type 4231 sound calibrator, and

the input channels of the interfaces were calibrated using a voltage calibrator. The input-to-output latency was removed according to a loopback measurement. To cut the impulse responses to the length defined in the scene description, the last 1024 samples were faded out using a one-sided Hann window. Details about the hardware used for each scene and the final impulse response lengths can be found in Table 3, Appendix A, and Appendix B.

Reference scenes. RS1–7 were measured with a G.R.A.S. 40AF free field compensated microphone capsule and the Genelec 8020c.

Complex rooms. CR1–4 were measured with a diffuse field compensated B&K 4134 capsule, the Genelec 8020c, and the dodecahedral speaker. For CR2–4, source and receiver positions and characteristics were chosen according to the requirements of ISO-3382-1 [30]. The measured IRs using the omnidirectional dodecahedron source thus allow the processing of most of the room acoustical parameters. A Matlab script for calculating C_{80} , D_{50} , EDT or T_{20} (among other parameters) using the *ita_roomacoustics* method of the ITA-Toolbox [4] is part of the BRAS.

3.4.2 Binaural Receiver

BRIRs were measured with the FABIAN head and torso simulator [31], the Genelec 8020c, and the QSC-K8 using swept sines and spectral deconvolution. The sweep length and level was adjusted to obtain SNRs of about 90 dB for a source in front of FABIAN, except at RS5, where a reduced SNR of 70 dB is due to the energy loss caused by the blocked direct sound path. FABIAN is equipped with DPA 4060 miniature electret condenser microphones located at the blocked ear channel entrances, and a computer controllable neck joint (Amtec Robotics PW-070, precision $\pm 0.02^\circ$) that was used to obtain BRIRs for head orientations of $\pm 44^\circ$ in steps of 2° to cover a typical range of motion, and allow for an artifact free dynamic auralization of head rotations [25, 26].

In post-processing, the smallest common propagation delay was removed from all BRIRs to minimize the latency in auralizations. This was done separately for each scene to assure that propagation delay differences between loudspeaker positions and HATOs remained as they were. A band pass filter was applied to suppress noise (4th order Butterworth, -3 dB @ 50 Hz/20 kHz). The on-axis magnitude response of FABIAN’s DPA microphones was removed to provide an uncolored on-axis frequency response for auralization by applying minimum phase inverse filters with a length of 128 samples. Afterwards the impulse responses were truncated at the position where the noise floor became visible and squared sine fades were applied to avoid discontinuities at the start and beginning. In a last step, the BRIRs were normalized using a single gain factor per scene, thus maintaining interaural level differences and relative level differences

between BRIRs for different speakers and HATOs. To obtain the gain factor, the BRIR measured with the speaker closest to FABIAN (with neutral head orientation) was averaged between 300 Hz and 1 kHz and across the left and right ear using AKtools [28]:

```
[~,~,gain] = AKnormalize(brir_lr, 'abs',
'mean', 'mean', 1, [300 1000]);
```

For the audio content provided in the database (anechoic string quartet, see Section 2.4) the bandwidth is sufficient, with C2 being the lowest playable note on a Cello with a fundamental frequency of 65 Hz. For other stimuli, the 50 Hz limit could indeed be a restriction. In these cases, the the same band-pass filter should be applied to the simulation.

Reference scenes. In RS1, 3, and 5 BRIRs were measured for selected positions of the Genelec 8020c.

Complex rooms. BRIRs were measured for selected positions of the Genelec 8020c in CR1. In CR2–4 a single receiver position was used and the QSC-K8 speaker was set up at five different positions to mimic a string quartet with a singer. For this purpose, the speakers were arranged in a hemi-circle with a radius of 1.5 m at positions of $\pm 90^\circ$ (1st violin, cello) and $\pm 30^\circ$ (2nd violin, viola), and tweeter heights of 103 cm (violins, viola) and 81 cm (cello). To realize the tilting and tweeter heights, the speakers were placed on a chair on top of a box (flight case filled with a layer of porous absorbers). A 3D model of the setup including the box, chair and loudspeaker is contained in the database (cf. Section 2.1.1). The speaker that mimicked the singer was placed on a stand in the center of the semi-circle with a tweeter height of 1.5 m. Except for the center, the speakers were rotated and tilted until the tweeter pointed towards FABIAN’s head (the position and orientation of the speaker was identical for all measured head orientations). BRIRs for the five source positions were measured one after another to avoid reflections from other speakers. Parametric equalizers were used to provide an uncolored on-axis frequency response of the QSC-K8 for auralization as described in section 3.3.1.

Acknowledgements

We would like to thank Thomas Maintz, Rob Opdam, Philipp Eschbach, Ingo Witew, Johannes Klein, and the workshop of the Institute of Technical Acoustics at RWTH Aachen University; Hannes Helmholtz, and Omid Kokabi from the Audio Communication Group at TU Berlin for assistance during the compilation of the BRAS database, and Oliver Strauch for measuring the directivity of the QSC-K8.

References

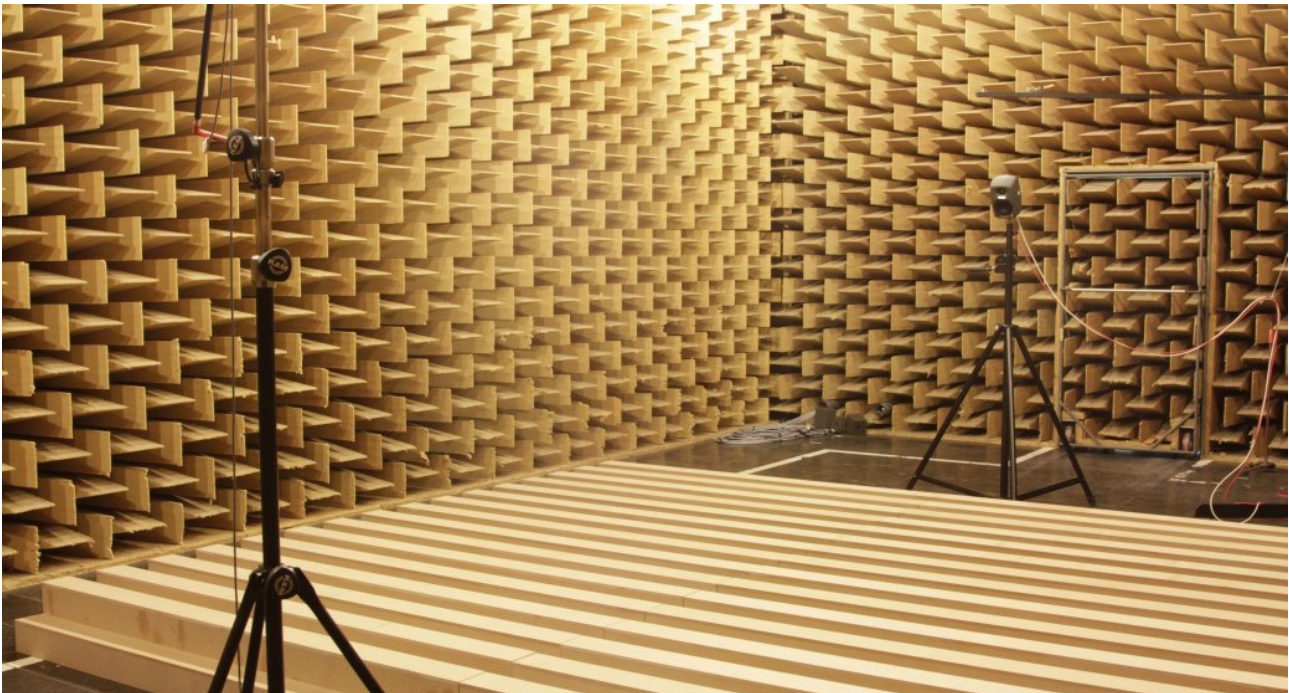
- [1] AES Standards Committee, *AES69-2015: AES standard for file exchange - Spatial acoustic data file format*. Audio Engineering Society, Inc., 2015.
- [2] F. Brinkmann, A. Lindau, S. Weinzierl, G. Geissler, S. van de Par, M. Müller-Trapet, R. Opdam, and M. Vorländer, “The FABIAN head-related transfer function data base,” DOI: 10.14279/depositonce-5718.3, Feb. 2017.
- [3] H. Kuttruff, *Room acoustics*, 5th ed. Oxford, UK: Spon Press, 2009.
- [4] M. Berzborn, R. Bomhardt, J. Klein, J.-G. Richter, and M. Vorländer, “The ITA-Toolbox: An open source MATLAB toolbox for acoustic measurements and signal processing,” in *Fortschritte der Akustik – DAGA 2017*, Kiel, Germany, Mar. 2017, pp. 222–225.
- [5] S. Müller and P. Massarani, “Transfer function measurement with sweeps. directors cut including previously unreleased material and some corrections,” *J. Audio Eng. Soc.* (Original release), vol. 49, no. 6, pp. 443–471, Jun. 2001.
- [6] A. Andreopoulou and B. F. G. Katz, “Identification of perceptually relevant methods of interaural time difference estimation,” *J. Acoust. Soc. Am.*, vol. 142, no. 2, pp. 588–598, Aug. 2017.
- [7] B. Bernschütz, “A spherical far field HRIR/HRTF compilation of the Neumann KU 100,” in *AIA-DAGA 2013, International Conference on Acoustics*, Merano, Italy, Mar. 2013, pp. 592–595.
- [8] P. Cignoni, C. Rocchini, and R. Scopigno, “Metro: Measuring error on simplified surfaces,” *Computer Graphics Forum*, vol. 17, no. 2, pp. 167–174, 1998.
- [9] M. Vorländer, *Auralization. Fundamentals of acoustics, modelling, simulation, algorithms and acoustic virtual reality*, 1st ed. Berlin, Heidelberg, Germany: Springer, 2008.
- [10] ISO 10534-2, *Determination of sound absorption coefficient and impedance in impedance tubes – Part 2: Transfer-function method*. Geneva, Switzerland: International Organization for Standards, Nov. 1998.
- [11] E. Mommertz, “Angle-dependent in-situ measurements of reflection coefficients using a subtraction technique,” *Applied Acoustics*, vol. 46, no. 3, pp. 251 – 263, 1995, building Acoustics.
- [12] Physikalisch-Technische Bundesanstalt (PTB), “Tabularized absorption and scattering values,” https://www.ptb.de/cms/fileadmin/internet/fachabteilungen/abteilung_1/1.6_schall/1.63/abstab_wf.zip (last checked Mar. 2019), 2012.

- [13] M. Müller-Trapet, P. Dietrich, M. Aretz, J. van Gemmeren, and M. Vorländer, “On the in situ impedance measurement with pu-probes — Simulation of the measurement setup,” *J. Acoust. Soc. Am.*, vol. 134, no. 2, pp. 1082–1089, Aug. 2013.
- [14] E. Tijs, “Study and development of an in situ acoustic absorption measurement method,” Ph.D. dissertation, University of Twente, Enschede, The Netherlands, Apr. 2013.
- [15] ISO 17497-1, *Sound-scattering properties of surfaces. Part 1: Measurement of the random-incidence scattering coefficient in a reverberation room*. Geneva, Switzerland: International Organization for Standards, May 2004.
- [16] ISO 17497-2, *Sound-scattering properties of surfaces. Part 2: Measurement of the directional diffusion coefficient in a free field*. Geneva, Switzerland: International Organization for Standards, May 2012.
- [17] B. N. J. Postma and B. F. G. Katz, “Creation and calibration method of acoustical models for historic virtual reality auralizations,” *Virtual Reality*, vol. 19, pp. 161–180, Sep. 2015.
- [18] G. Behler and M. Vorländer, “An active loudspeaker point source for the measurement of high quality wide band room impulse responses,” in *Proceedings of the Institute of Acoustics – Auditorium Acoustics 2018*, vol. 40, no. 3. Hamburg, Germany: Institute of Acoustics, 2018, pp. 435–446. [Online]. Available: https://www.dega-akustik.de/fileadmin/dega-akustik.de/DEGA/aktuelles/IOA_AA_Program.pdf
- [19] T. W. Leishman, S. Rollins, and H. M. Smith, “An experimental evaluation of regular polyhedron loudspeakers as omnidirectional sources of sound,” *J. Acoust. Soc. Am.*, vol. 120, no. 3, pp. 1411–1422, Sep. 2006.
- [20] R. Bristow-Johnson, “The equivalence of various methods of computing biquad coefficients for audio parametric equalizers,” in *97th AES Convention, Preprint*, San Francisco, USA, Nov. 1994.
- [21] M. Möser, *Engineering acoustics: An Introduction to noise control*, 2nd ed. Berlin Heidelberg: Springer, 2009.
- [22] D. B. Keele Jr., “Low-frequency loudspeaker assessment by nearfield sound-pressure measurement,” *J. Audio Eng. Soc.*, vol. 22, no. 3, pp. 154–162, Apr. 1974.
- [23] B. Rafaely, *Fundamentals of spherical array processing*, 1st ed. Berlin, Heidelberg, Germany: Springer, 2015.
- [24] F. Brinkmann, A. Lindau, S. Weinzierl, S. v. d. Par, M. Müller-Trapet, R. Opdam, and M. Vorländer, “A high resolution and full-spherical head-related transfer function database for different head-above-torso orientations,” *J. Audio Eng. Soc.*, vol. 65, no. 10, pp. 841–848, Oct. 2017.
- [25] W. R. Thurlow, J. W. Mangels, and P. S. Runge, “Head movements during sound localization,” *J. Acoust. Soc. Am.*, vol. 42, no. 2, pp. 489–493, 1967.
- [26] A. Lindau and S. Weinzierl, “On the spatial resolution of virtual acoustic environments for head movements on horizontal, vertical and lateral direction,” in *EAA Symposium on Auralization*, Espoo, Finland, Jun. 2009.
- [27] F. Brinkmann, R. Roden, A. Lindau, and S. Weinzierl, “Audibility and interpolation of head-above-torso orientation in binaural technology,” *IEEE J. Sel. Topics Signal Process.*, vol. 9, no. 5, pp. 931–942, Aug. 2015.
- [28] F. Brinkmann and S. Weinzierl, “AKtools – An open software toolbox for signal acquisition, processing, and inspection in acoustics,” in *142nd AES Convention, Convention e-Brief 309*, Berlin, Germany, May 2017.
- [29] B. N. J. Postma and B. F. G. Katz, “Correction method for averaging slowly time-variant room impulse response measurements,” *J. Acoust. Soc. Am.*, vol. 140, no. 1, pp. EL38–EL43, 2016.
- [30] ISO 3382-1, *Measurement of room acoustic parameters – Part 1: Performance spaces*. Geneva, Switzerland: International Organization for Standards, 2009.
- [31] A. Lindau, T. Hohn, and S. Weinzierl, “Binaural resynthesis for comparative studies of acoustical environments,” in *122th AES Convention, Convention Paper 7032*, Vienna, Austria, May 2007.
- [32] F. Brinkmann, M. Dinakaran, R. Pelzer, P. Grosche, D. Voss, and S. Weinzierl, “A cross-evaluated database of measured and simulated HRTFs including 3D head meshes, anthropometric features, and headphone impulse responses,” *J. Audio Eng. Soc. (Engineering Report)*, vol. 67, no. 9, pp. 705–718, Sep. 2019.
- [33] L. Aspöck, F. Brinkmann, D. Ackerman, S. Weinzierl, and M. Vorländer, “GRAS – Ground Truth for Room Acoustical Simulation,” DOI: [10.14279/depositonce-6726](https://doi.org/10.14279/depositonce-6726), Mar. 2018.
- [34] —, “BRAS – Benchmark for Room Acoustical Simulation,” DOI: [10.14279/depositonce-6726.2](https://doi.org/10.14279/depositonce-6726.2), May 2019.

- [35] —, “BRAS – Benchmark for Room Acoustical Simulation,” DOI: [10.14279/depositonce-6726.3](https://doi.org/10.14279/depositonce-6726.3), Apr. 2020.

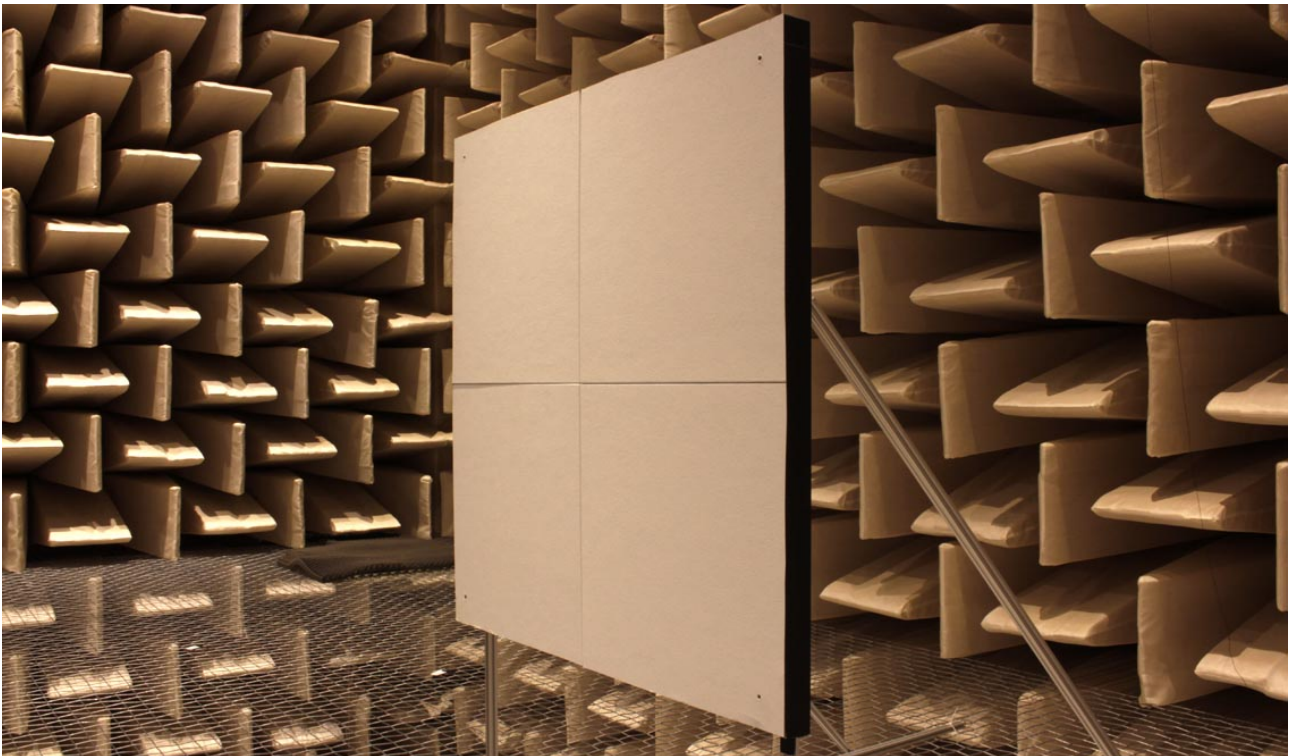
BRAS: Reference scenes

RS1: Simple reflection (infinite plate)



Short description:	Simple reflection on three different (infinite) surfaces: Hard floor of hemi anechoic chamber, RockFon absorber and medium density fiber-board (MDF) diffusor. Monaural impulse responses for three loudspeaker positions and angles (30°,45°, 60°) and three microphone positions. Binaural impulse responses for one loudspeaker position and one receiver position.
Room:	Hemi anechoic chamber RWTH Aachen ($V = 296 \text{ m}^3$, $f_{\text{low}} = 100 \text{ Hz}$)
Temperature:	20.3 °C
Humidity:	41.5 %
Sampling rate:	44100 Hz
Scene geometry:	RS1_RIR_Floor.skp RS1_RIR_Absorber.skp RS1_RIR_Diffusor.skp RS1_BRIR_Floor.skp RS1_BRIR_Absorber.skp RS1_BRIR_Diffusor.skp
Output IRs:	29 RIRs; 3 BRIR sets (11,025 samples duration)
Comment(s):	For a more detailed description of the reflecting objects, see *.skp files in the folder <i>AdditionalSceneDescription</i> .

RS2: Simple reflection and diffraction (finite plate)



Short description: Simple reflection and diffraction on, and around finite square boards with edge length of 1 m, and 2 m, rigid and absorbing surface, and multiple angles of sound incidence (30°, 45°, 60°). Plates were of medium density fiberboard (MDF) with a thickness of 25 mm. As absorbing material, Rockfon SONAR-G with a thickness of 20 mm was glued to the plate.

Room: Fully anechoic chamber TU Berlin ($V = 1070 \text{ m}^3$, $f_{\text{low}} = 63 \text{ Hz}$)

Temperature: 17.6 °C

Humidity: 47 %

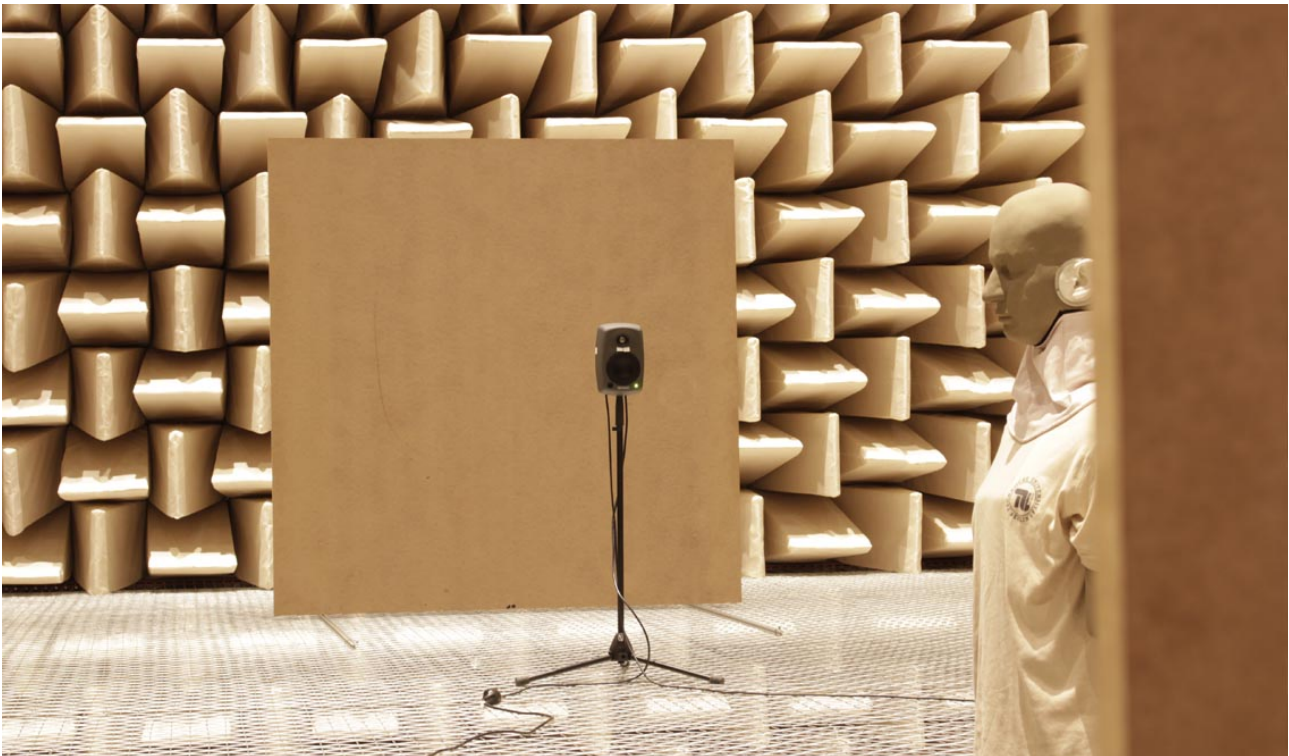
Sampling rate: 44100 Hz

Scene geometry: RS2_RIR_1mPlate_Rigid.skp
RS2_RIR_1mPlate_Absorbing.skp
RS2_RIR_2mPlate_Rigid.skp
RS2_RIR_2mPlate_Absorbing.skp

Output IRs: 18 RIRs; 0 BRIRs (6,000 samples duration)

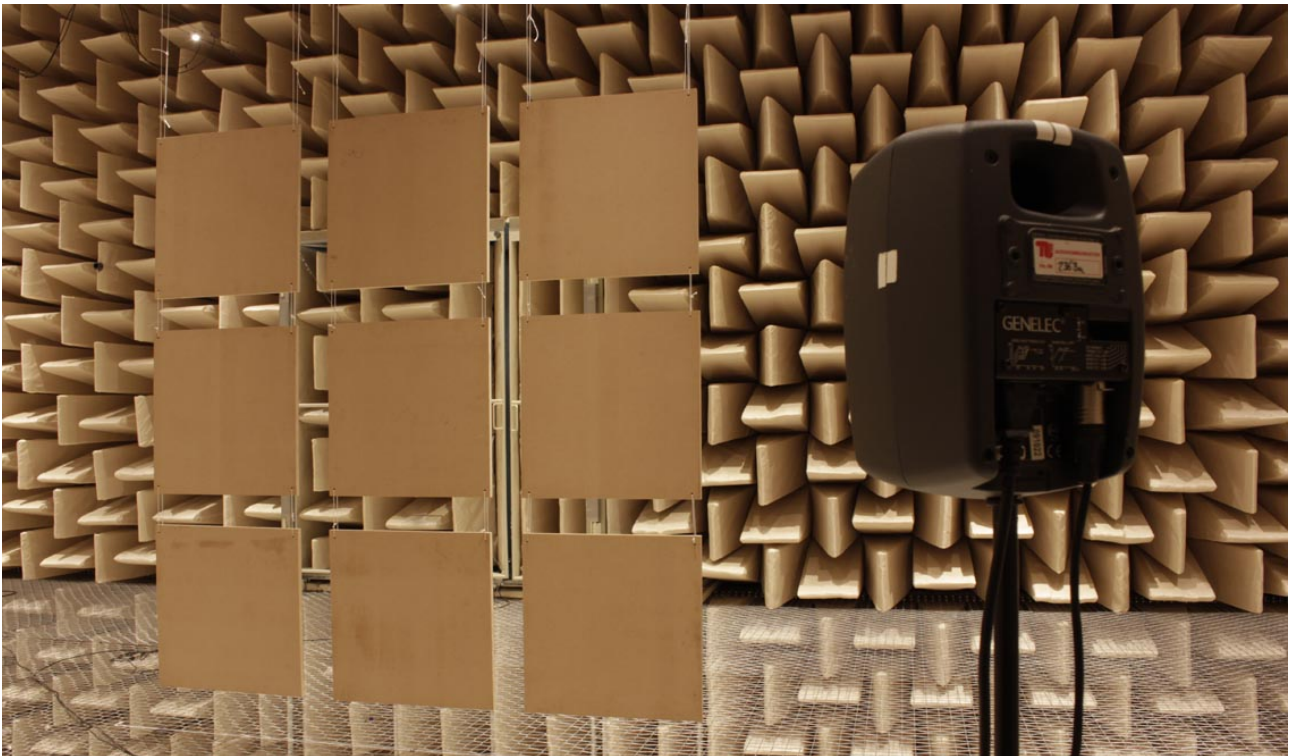
Comment(s): Due to logistical reasons diffraction was not measured for the 2 m plate with the absorbing surface. Sound transmission can be approximated based on density of the reflector plate, provided in the material description file *mat.MDF25mmA_plane*. The supporting structure, that holds the reflector, was included in the scene geometry for completeness, but might be removed for acoustical simulation.

RS3: Multiple reflection (finite plate)



- Short description:** Multiple reflections between two finite square boards with edge length of 2 m, and rigid surfaces. Plates were of medium density fiberboard (MDF) with a thickness of 25 mm.
- Room:** Fully anechoic chamber TU Berlin ($V = 1070 \text{ m}^3$, $f_{\text{low}} = 63 \text{ Hz}$)
- Temperature:** 17.3 °C
- Humidity:** 49.5 %
- Sampling rate:** 44100 Hz
- Scene geometry:** RS3.RIR.skp
RS3.BRIR.skp
- Output IRs:** 1 RIRs; 1 BRIR set (50,000 samples duration)
- Comment(s):** Sound transmission can be approximated based on density of the reflector plate, provided in the material description file *mat_MDF25mmA_plane*. The supporting structure, that holds the reflector, was included in the scene geometry for completeness, but might be removed for acoustical simulation.

RS4: Simple reflection (reflector array)



Short description: Simple reflection on a reflector array with rigid surfaces, and for multiple angles of sound incidence (30° , 45° , 60°). The loudspeaker was positioned to aim at the center of the array (on-center), and between two plates (off-center). Plates were of medium density fiberboard (MDF) with an edge length of 68 cm, and a thickness of 25 mm.

Room: Fully anechoic chamber TU Berlin ($V = 1070 \text{ m}^3$, $f_{\text{low}} = 63 \text{ Hz}$)

Temperature: 17.6 °C

Humidity: 45.5 %

Sampling rate: 44100 Hz

Scene geometry: RS4_onCenter.skp
RS4_offCenter.skp
RS4_sketch.pdf

Output IRs: 18 RIRs; 0 BRIRs (8,000 samples duration)

Comment(s): The SketchUp files show the actual geometry of the reflector array. The intended geometry of a perfectly even spaced array could not be met, however, deviations are below 1 cm in most of the cases (cf. RS4_sketch.pdf). The reflector array was hung from the ceiling with cords. Sound transmission can be approximated based on density of the reflector plates, provided in the material description file *mat_MDF25mmA_plane*.

RS5: Simple diffraction (infinite edge)



Short description: Simple diffraction at a partition (25mm MDF) with a height of 2.07 m. Monaural impulse responses for four loudspeaker and four microphone positions (different heights). Binaural impulse responses for one loudspeaker position and one receiver position.

Room: Hemi anechoic chamber RWTH Aachen
($V = 296 \text{ m}^3$, $f_{\text{low}} = 100 \text{ Hz}$)

Temperature: 20.3 °C

Humidity: 40.3 %

Sampling rate: 44100 Hz

Scene geometry: RS5_RIR.skp
RS5_BRIR.skp

Output IRs: 16 RIRs; 1 BRIR set (11,025 samples duration)

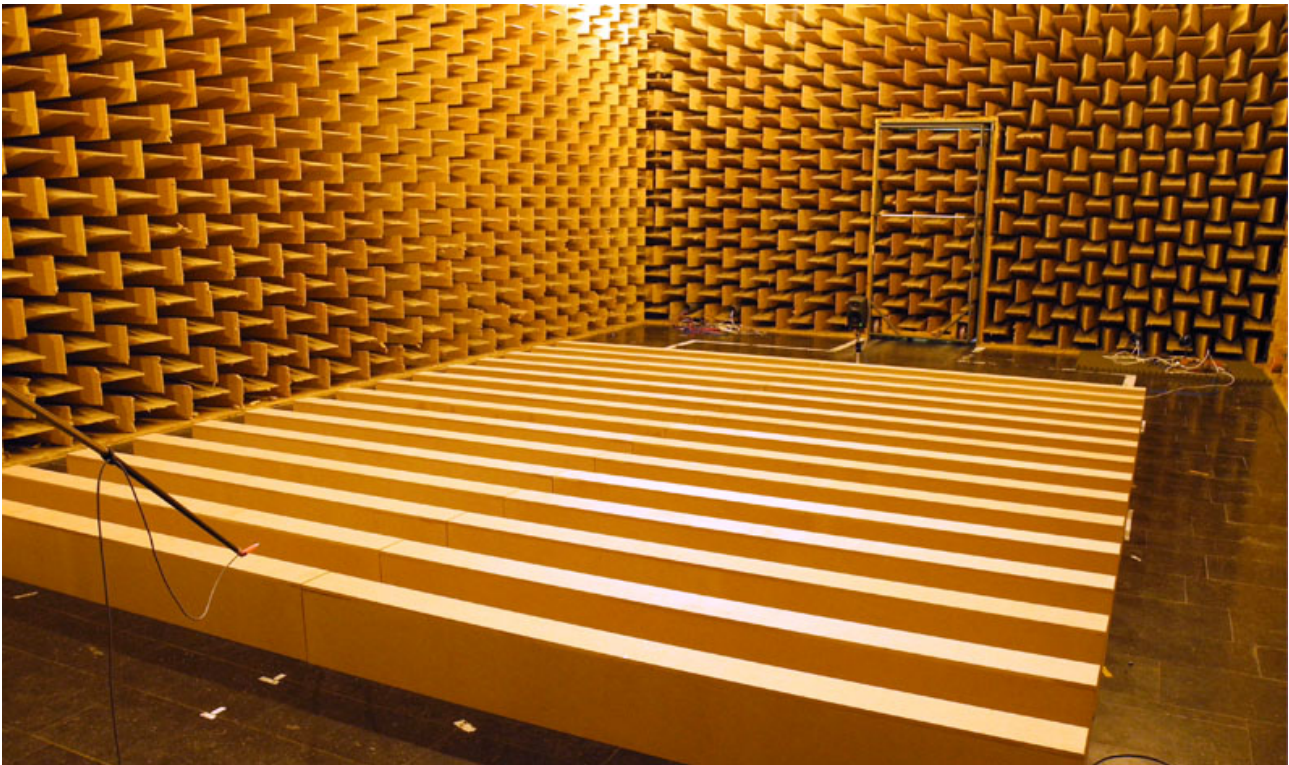
Comment(s): Sound transmission can be approximated based on the density of the partition, provided in the material description file *mat_MDF25mmB_plane*.

RS6: Diffraction (finite body)



- Short description:** Diffraction around a cubic body made of 18 hollow wooden blocks (12mm MDF) with a total height and depth of 0.72 m and a width of 4.14 m. Monaural impulse responses for three loudspeaker and three microphone positions (different heights).
- Room:** Hemi anechoic chamber RWTH Aachen
($V = 296 \text{ m}^3$, $f_{\text{low}} = 100 \text{ Hz}$)
- Temperature:** 19.9 °C
- Humidity:** 40.1 %
- Sampling rate:** 44100 Hz
- Scene geometry:** RS6_RIR.skp
- Output IRs:** 9 RIRs, 0 BRIRs (11,025 samples duration)
- Comment(s):** Sound transmission can be approximated based on the density of the wood, provided in the material description file *mat_MDF12mm_plane*. Note that the body is set up by separated components, check the scene description file for details.

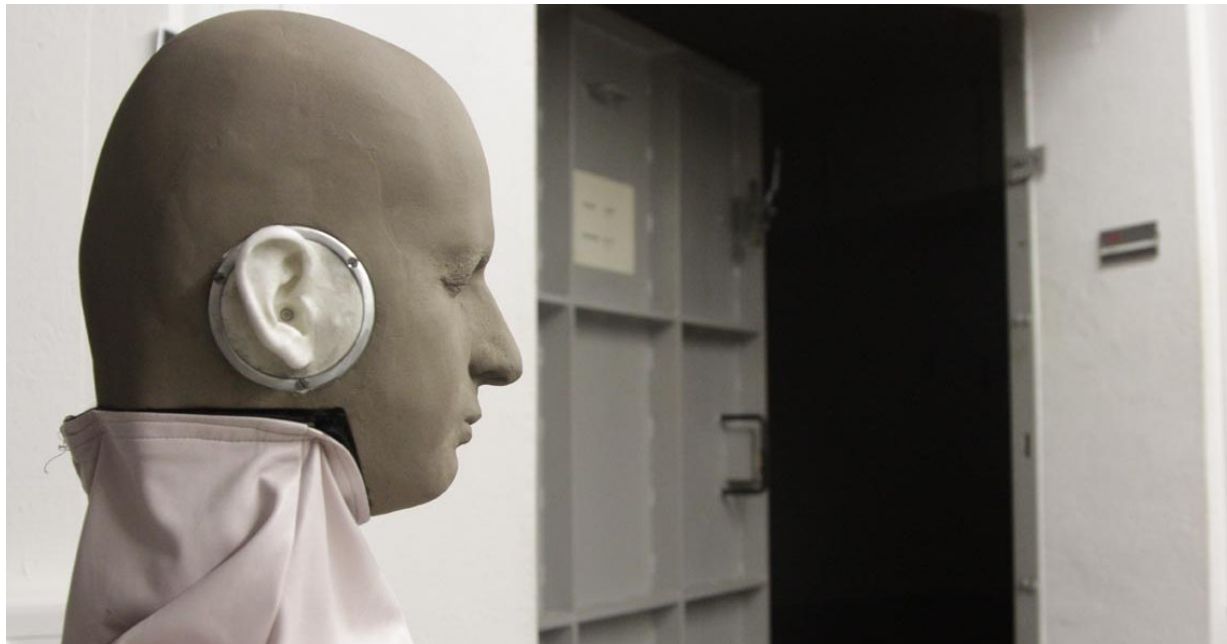
RS7: Multiple diffraction (seat dip effect)



- Short description:** Seat dip like diffraction around 15 cubic blocks with a height of 0.24 m, depth of 0.12 m, and a width of 4.1 m (made from 12mm MDF). Spacing between blocks is 0.22 m. Monaural impulse responses for two loudspeaker and four microphone positions (different heights).
- Room:** Hemi anechoic chamber RWTH Aachen
($V = 296 \text{ m}^3$, $f_{\text{low}} = 100 \text{ Hz}$)
- Temperature:** 19.2 °C
- Humidity:** 40.3 %
- Sampling rate:** 44100 Hz
- Scene geometry:** RS7_RIR.skp
- Output IRs:** 8 RIRs, 0 BRIRs (11,025 samples duration)
- Comment(s):** Sound transmission can be approximated based on the density of the wood, provided in the material description file *mat_MDF12mm_plane*.

Appendix: Complex rooms

CR1: Coupled rooms (laboratory & reverberation chamber)



Short description: A simple case of coupled rooms where a reverberation chamber is coupled to a laboratory room with a lower reverberation time. The scene was measured for two different opening angles of the door (DoorAngle1=4.1°, DoorAngle3=30.4°) for the door between the rooms.

Volume: 122 m³ + 104 m³ (reverberation chamber + laboratory room)

Temperature: 18.2 °C

Humidity: 47.6 %

Sampling rate: 44100 Hz

Scene geometry: CR1_RIR_DoorAngle1.skp
CR1_RIR_DoorAngle3.skp
CR1_BRIR_01_DoorAngle3.skp
CR1_BRIR_02_DoorAngle3.skp
CR1_TW1.skp (geometry only)
CR1_TW3.skp (geometry only)

Output IRs: 40 RIRs; 2 BRIR sets (198,450 samples duration – 4.5 s)

RIRs for the Genelec 8020c were measured for 4 orientations with the following labels and x/y/z orientation vectors according to the scene's global coordinate system:

01: [-0.6552 0.7555 0]

02: [-0.7555 -0.6552 0]

03: [0.6552 -0.7555 0]

04: [0.7555 0.6552 0]

WARNING: The level of the RIRs was manually corrected by 6 dB to meet the expected direct sound level.

CR2: Small room (seminar room)



Short description: The seminar room at Aachen University was chosen for the small room because its relatively simple and easy to describe geometry, but challenging low frequency behaviour.

Volume: 145 m³

Temperature: 19.5 °C

Humidity: 41.7 %

Sampling rate: 44100 Hz

Scene geometry: CR2_RIR.skp
CR2_BRIR.skp
CR2.skp (geometry only)

Output IRs: 49 RIRs; 5 BRIR sets (154,350 samples duration – 3.5 s)

RIRs for the Genelec 8020c were measured for 4 orientations with the following labels and x/y/z orientation vectors according to the scene's global coordinate system:

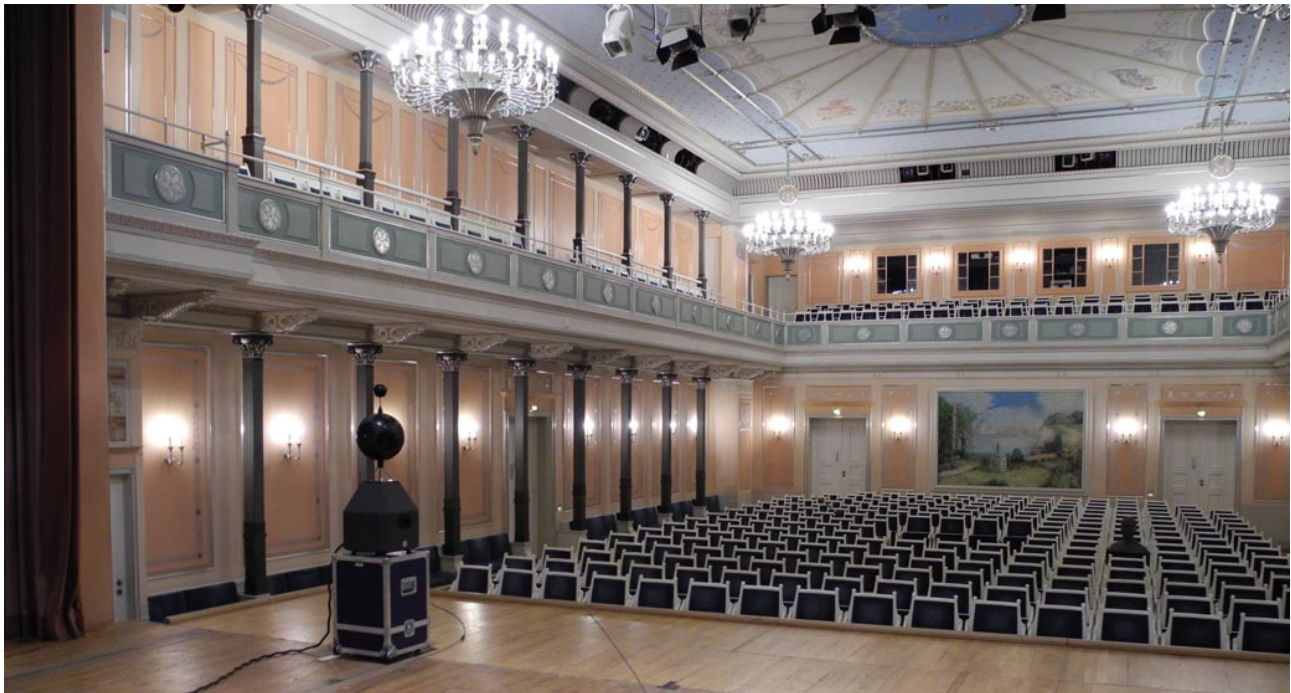
positiveX: [1 0 0]

positiveY: [0 1 0]

negativeX: [-1 0 0]

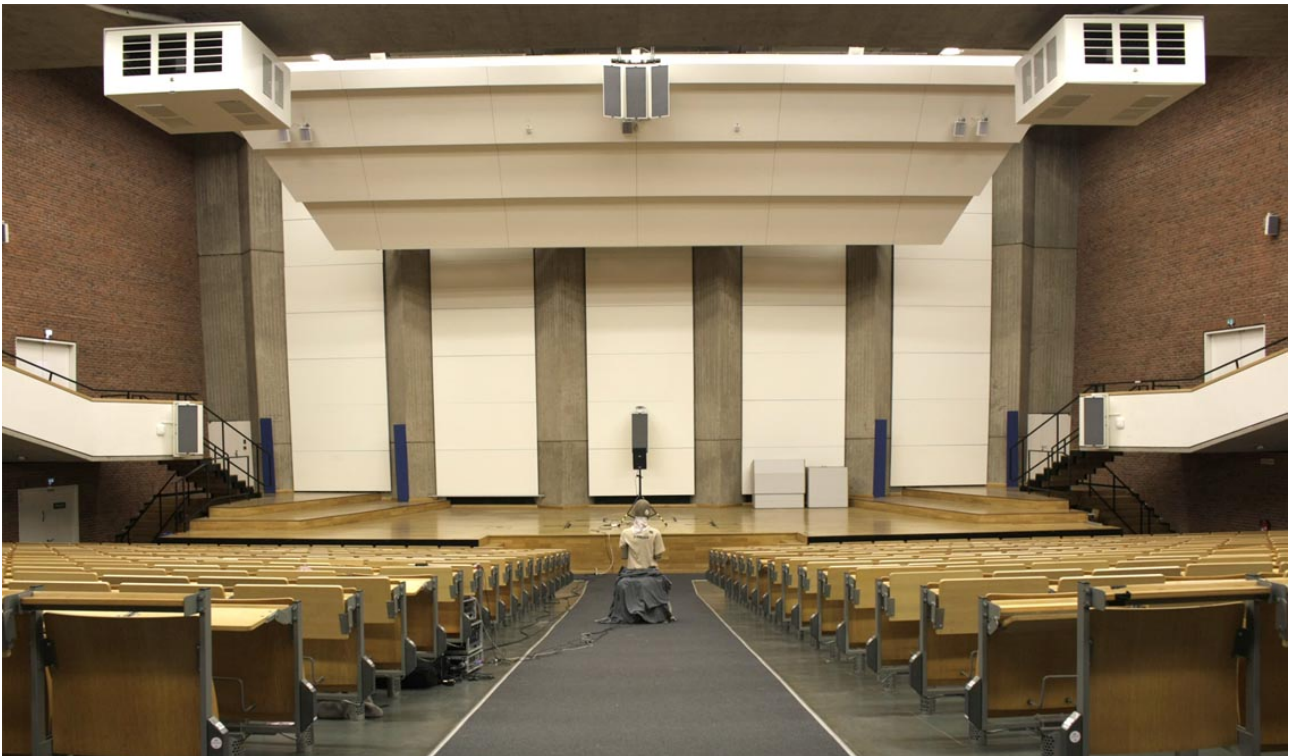
negativeY: [0 -1 0]

WARNING: The level of the RIRs was manually corrected by 6 dB to meet the expected direct sound level. The RIR of the Genelec 8020c speaker for LS1 (orientation positive Y) MP5 is missing.

CR3: Medium room (chamber music hall)

- Short description:** The small hall of the Konzerthaus Berlin was chosen for the medium room because of its relevance for chamber music and its relatively simple and easy to describe geometry.
- Volume:** 2,350 m³ (excluding the attic volume)
- Temperature:** 22.4 °C
- Humidity:** 40.9 %
- Sampling rate:** 44100 Hz
- Scene geometry:** CR3_RIR.skp
CR3_BRIR.skp
CR3.skp (geometry only)
- Output IRs:** 70 RIRs; 5 BRIR sets (154,350 samples duration – 3.5 s)
RIRs for the Genelec 8020c were measured for 4 orientations with the following labels and x/y/z orientation vectors according to the scene's global coordinate system:
positiveX: [1 0 0]
positiveY: [0 1 0]
negativeX: [-1 0 0]
negativeY: [0 -1 0]
- Comment(s):** The room has a considerable volume above its ceiling, which is included in the 3D model and might be excluded or simplified for acoustic simulation. The volume is coupled by large connections at the stage, and small connections on the ceiling.
- WARNING:** The level of the RIRs was manually corrected by 6 dB to meet the expected direct sound level.

CR4: Large room (auditorium)



Short description: The Auditorium Maximum at TU Berlin was chosen for the large room because of its relatively simple and easy to describe geometry.

Volume: 8,650 m³

Temperature: 20.9 °C

Humidity: 37.5 %

Sampling rate: 44100 Hz

Scene geometry: CR4_RIR.skp
CR4_BRIR.skp

CR4.skp (geometry only)

Output IRs: 50 RIRs; 5 BRIR sets (154,350 samples duration – 3.5 s)

RIRs for the Genelec 8020c were measured for 4 orientations with the following labels and x/y/z orientation vectors according to the scene's global coordinate system:

positiveX: [1 0 0]

positiveY: [0 1 0]

negativeX: [-1 0 0]

negativeY: [0 -1 0]

Comment(s): The model provides a high degree of detail that can be reduced depending on the needs of each participant.

WARNING: The level of the RIRs was manually corrected by 6 dB to meet the expected direct sound level.

Version History

A first non-public version of the database was created in 2016 to provide input data to the participants of a round robin investigation on room acoustic simulation and auralization [32]. At this stage, the database did not include the measured impulse responses. The measurements were added to the database in the public release in 2018 [33]. This version of the database was initially called *Ground Truth for Room Acoustical Simulation* (GRAS), but was later renamed and published as the *Benchmark for Room Acoustical Simulation* (BRAS) [34] to reflect the measurement uncertainty of the complex rooms. Internal revisions and peer-reviews of related publications helped to improve and extend the database, leading to the most recent version [35]. An overview of the versions, changes, and additions to the database is given in Table 6.

1	Round robin database: non-public, 2016 [32] - initial version without measured impulse responses
2	GRAS: Version 1, 2018, DOI: 10.14279/depositonce-6726 [33] - added reference scenes 6 and 7 (RS6 and RS7) - added measured impulse responses for all scenes - correction of some scene descriptions
3	BRAS: Version 2, 2019, DOI: 10.14279/depositonce-6726.2 [34] - first major update: Renaming and revision of database - general update of documentation and surface descriptions - correction of minor mistakes in scene descriptions - added <i>fitted</i> absorption coefficients for complex rooms - added detailed photo documentation for complex rooms - added geometric details of 3D models in scenes 9, 10 and 11 (now CR2–4) - added more detailed description of dodecahedron speaker - added directivity data of dodecahedron speaker
4	BRAS: Version 3, 2020, DOI: 10.14279/depositonce-6726.3 [35] - general update of documentation - renamed scenes 1-7 to reference scenes 1–7 (RS1–7) - renamed scenes 8-11 to complex rooms 1–4 (CR1–4) - added list of 3D model simplifications for complex rooms - updated surface description and scattering coefficients - removed source and receiver directivities given in mat-files - added a Matlab script for reading directivities given in csv-files - correction of minor mistakes in scene descriptions

Table 6: History of the database.